# Oxide superlattices with alternating $p$ and $n$ interfaces

N. C. Bristowe,[1,2] Emilio Artacho,[2] and P. B. Littlewood[1]

[1] *Theory of Condensed Matter Group,*
*Cavendish Laboratory, University of Cambridge,*
*JJ Thomson Ave, Cambridge CB3 0HE, UK*

[2] *Department of Earth Sciences, University of Cambridge,*
*Downing Street, Cambridge CB2 3EQ, UK*

(Dated: July 7, 2009)

## Abstract

The physics of oxide superlattices is considered for pristine (001) multilayers of the band insulators $LaAlO_3$ and $SrTiO_3$ with alternating $p$ and $n$ interfaces. A model of charged capacitor plates offers a simple paradigm to understand their dielectric properties and the insulator to metal transition (IMT) at interfaces with increasing layer thickness. The model is supported by first-principles results based on density-functional theory. The charge at insulating interfaces is argued and found to be as predicted from the formal ionic charges, not populations. Different relative layer thicknesses produce a spontaneous polarization of the system, and allow manipulation of the interfacial electron gas. Large piezoresistance effects can be obtained from the sensitivity of the IMT to lateral strain. Carrier densities are found to be ideal for exciton condensation.

PACS numbers: 73.21.Cd, 71.30.+h, 73.20.-r

Keywords:

## I. INTRODUCTION

Recent technological advances have enabled the fabrication of high quality oxide multilayers, revealing a wealth of fascinating new physics. One striking example is the $LaAlO_3/SrTiO_3$ system (LAO/STO). In 2004, Ohtomo and Hwang[1] discovered that the interface between these two perovskite band insulators can be conducting, depending on the termination of both materials. Many experimental and theoretical studies have followed[2–17]. Charge compensation at the interface of thick layers is required to avoid the so-called polar catastrophe. It arises from the diverging electrostatic potential caused by the net electric charge at these interfaces resulting from the fact that the (001) monolayers of STO are neutral while the ones of LAO are charged. The $TiO_2$-LaO interface (termed $n$) needs 0.5 electrons per two-dimensional (2D) unit cell, and the SrO-$AlO_2$ interface ($p$) 0.5 holes to avoid this polar catastrophe. Such numbers are based on formal ionic charges, i.e., $Ti^{+4}$, $Sr^{+2}$, $La^{+3}$, $Al^{+3}$, and $O^{-2}$, although it is well known that the charge distribution in these materials is far from being so ideally ionic. Formal charges are often downscaled by so-called covalency parameters that aim to describe more realistic charges[18].

These compensating electrons and holes are confined to the interface regions, but highly mobile in 2D, defining 2D electron and hole gases[9,11]. Huijben *et al.*[2] (see[17] for the theory) studied a system with one $p$ and one $n$ interface, finding 2D conduction beyond a critical interface separation of five unit cells. Characteristics like carrier mobility depend on the carrier density, which grows with separation beyond the critical value[16]. Multilayers with both $p$ and $n$ interfaces with such a control of carrier density provide promising systems for obtaining the so-far elusive excitonic insulator[19]. Recent experiments have demonstrated that oxygen vacancies can be controlled, while still allowing metallic conduction attributed to a 2D layer [6,20].

This paper focuses on superlattices with alternating $p$ and $n$ interfaces. We consider pristine systems, with no point defects (the effect of oxygen vacancies[12,13] is discussed at the end). Considering an equal thickness for both materials, an IMT is found by our calculations based on density-functional theory (DFT) for a thickness of just over eight unit cells. The electrostatic potential obtained in the calculations agrees remarkably well with a simple model of capacitor plates, giving an almost constant field of opposite sign in both materials, which does not change with increasing thickness until the potential drop coincides with the

band gap. At that critical thickness electrons transfer from the $p$ to the $n$ interface, making them conducting, and pinning the potential drop.

## II. METHOD

The DFT calculations were done using the local density approximation[21] and the SIESTA method[22,23]. Norm-conserving pseudopotentials[24] were used, considering normal cores for O and Al, while semi-core electrons were included in the valence for La($5s5p$), Sr($4s4p$) and Ti($3s3p$). Double-$\zeta$ polarized bases were used for valence electrons[25]. Integrals in real space were performed on a mesh of 250 Ry cutoff[23], while Brillouin zone integrations were done on a $k$-mesh of 30 Å cutoff[26]. Four unit cells of STO in its ideal perovskite structure were layered on top of four of LAO, the 4/4 superlattice containing both $TiO_2$-LaO and SrO-$AlO_2$ terminations. The lateral lattice parameter was set to the theoretical average for the two materials. The cell size was relaxed perpendicular to the interface ($z$) along with the atomic positions until the forces were below 15 meV/Å. Samples for 8/8 and 12/12 unit cells were equally prepared. Other DFT studies [7–17], have focused on single interfaces of either kind, on arrays of repeated interfaces, or on alternating $p$ and $n$ interfaces. The latter[7,8,12] have considered four unit cells or less, too thin to observe the physics discussed here.

## III. RESULTS AND DISCUSSION

### A. Superlattice calculations

The band structures of the three superlattices are presented in Figure 1. The band gap is indirect and reduces with interface separation, closing for the 12/12 system, with holes and electrons separated in reciprocal space. The behavior in real space is shown in Figure 2 for the 12/12 case using the density of states projected onto each bilayer. The electrostatic potential is plotted alongside.

The physics of the problem is apparent in this figure. The net electric charge of chemical origin at the interfaces establish electric fields among them, defining a zig-zag potential, which is closely followed by the band structure of both materials. The IMT occurs when the amplitude of the zig-zag is larger than the band gap (the valence band offsets are small in this scale, 0.2 eV for the $p$ and 0.0 eV for the $n$ interfaces). At this point holes appear

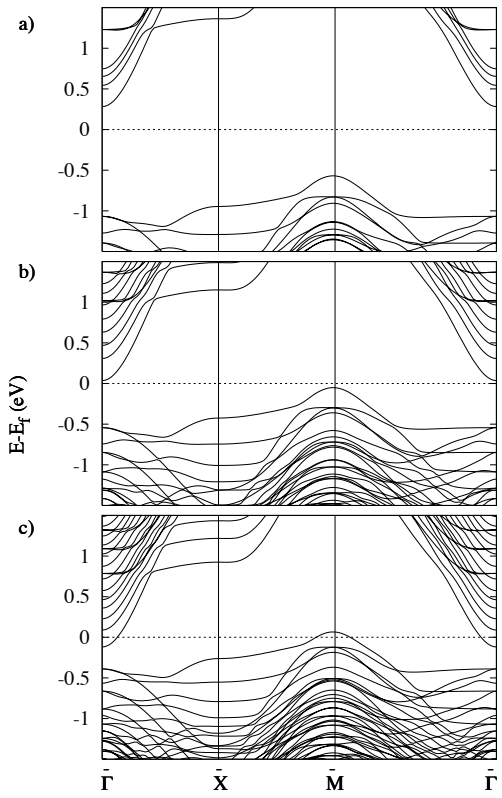


FIG. 1: Band structures of three $LaAlO_3/SrTiO_3$ superlattices with (a) 4/4, (b) 8/8, and (c) 12/12 unit-cell thicknesses.

confined in $z$ around the $AlO_2$ plane of the $p$ interface, and around the $\bar{M}$ point in the 2D Brillouin zone, while electrons are confined to the $TiO_2$ plane at the $n$ interface, and around $\bar{\Gamma}$. The 2D electron gas (2DEG) is dominated by a Ti $3d$ character. It is nicely parabolic with an effective mass of 0.4 $m_e$. The several parallel sub-bands at this interface correspond to excitations under the effective confining potential for electrons along $z$ (Fig. 4a)[39].

Quantitative predictions for the IMT are biased by the known band-gap problem of Kohn-Sham fermions[28]. Constrained DFT calculations as used for charge-transfer systems[29] can be used for ours, but are beyond the scope of this work, its focus being the elucidation of the main mechanisms at play. In addition, it has been argued that, being $LaTiO_3$ a system with highly correlated electrons in the Ti $3d$ band, methods addressing strong correlations are needed for our system. Note that this is not the case, however, since our IMT is in the limit of zero occupation of the $3d$ band, hardly a correlated system, unlike $LaTiO_3$, which has one $3d$ electron per Ti atom.

The deviations from the zig-zag behavior of the potential are small in the scale of its

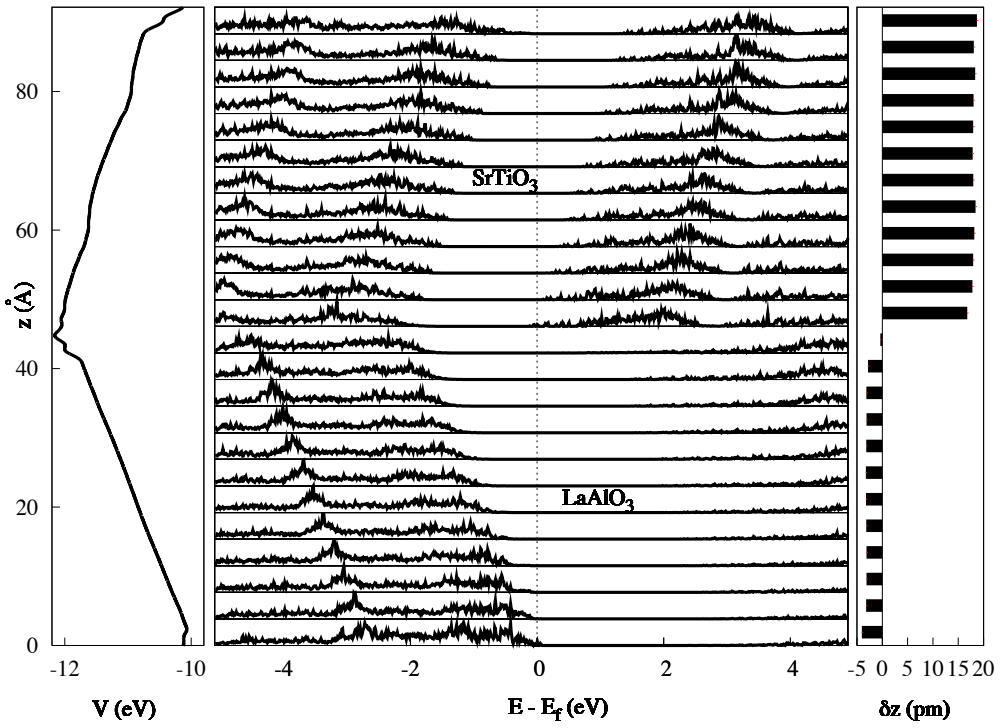


FIG. 2: Centre: Density of states projected on unit-cell bilayers for the 12/12 superlattice. Left: Averaged[27] electrostatic potential energy for electrons as a function of $z$. Right: The anion-cation splitting of the $TiO_2$ planes in $SrTiO_3$ and LaO planes in $LaAlO_3$ (larger splitting in each material), with $\delta z = z_{\text{cation}} - z_{\text{anion}}$.

amplitude, allowing the definition of a net electric field through each material. Its magnitude is nearly equal in both materials despite their different dielectric response. Such response is illustrated in Figure 2 by the $z$-splitting of cations and anions at each layer, which is much larger for STO as expected. The fields obtained are 57.3 mV/Å and 57.1 mV/Å for the 4/4 and 8/8 superlattices, while the 12/12 sees it reduced to 37.8 mV/Å due to the partial charge back-transfer. The field values correlate with the difference in sub-band separation seen in Figure 1. An estimate of the 2DEG width $W$ is obtained from $W \sim E_{ZPE}/\mathcal{E}$, i.e. the zero-point energy (ZPE) for the confining potential, over its slope, the electric field. Taking for 8/8, $\mathcal{E} = 57$ mV/Å and $E_{ZPE} \sim 0.2$ eV gives $W \sim 4$ Å.

### B. Model of charged plates

The physics described can be further analyzed with a simple model. The insulating system is modeled by a sequence of capacitor plates, one per interface, separated by dielectric material, as sketched in Figure 3. Each plate has a planar charge density of chemical origin $\sigma_c$ (the $0.5e$ per interface unit cell described above), positive at the $n$ interface, negative for the $p$. Using Gauss's law, periodic boundary conditions (PBC), and equal thicknesses, there is a uniform electric field of magnitude $\mathcal{E}^0$ pointing outwards from the $n$ interface that satisfies

$$\sigma_c - P_{\mathrm{LAO}} - P_{\mathrm{STO}} = 2\epsilon_0\mathcal{E}^0, \tag{1}$$

with $P_{\mathrm{LAO}}$ and $P_{\mathrm{STO}}$ the magnitude of the respective polarizations of both materials under the field, and $\epsilon_0$ the dielectric permittivity of vacuum. The left hand side is what is indicated by $\sigma_{\mathrm{net}}$ in Figure 3. The behavior at the $p$ interface is exactly opposite, with the field now pointing towards the plate. The fields have equal magnitude in both materials even if both polarizations are different.

Finding $\mathcal{E}^0$ requires knowing $P(\mathcal{E})$ beyond linear response, at least for STO. Under the strain conditions imposed by our geometry, the bulk of STO presents a spontaneous polarization along $z$[30,31], which allows a simpler modeling than for unstrained STO, and offers an upper bound in the response, which corresponds to an upper bound to the critical thickness for the IMT. We take $P_{\mathrm{LAO}} = \epsilon_0\chi_{\mathrm{LAO}}\mathcal{E}$ and $P_{\mathrm{STO}} = P^0_{\mathrm{STO}} + \epsilon_0\chi_{\mathrm{STO}}\mathcal{E}$. Defining $\kappa = 2 + \chi_{\mathrm{STO}} + \chi_{\mathrm{LAO}}$, equation 1 becomes

$$\mathcal{E}^0 = (\sigma_c - P^0_{\mathrm{STO}})/\epsilon_0\kappa. \tag{2}$$

We obtain $P^0_{\mathrm{STO}} = 0.309$ C/m$^2$ using the Berry phase approach[32] for bulk STO with the same strain conditions as in the multilayer. The lattice contribution to both susceptibilities is computed as in Ref. 31 from the phonons and the Born effective charges, which are obtained by finite differences of the forces and the polarization, respectively[33]. The computed susceptibilities are $\chi^{ph}_{33}$(LAO)= 12.2 and $\chi^{ph}_{33}$(STO)= 24.7. To these we add the electronic contribution taking it from $\epsilon^{\infty}$(STO)= 5.18[34] and $\epsilon^{\infty}$(LAO)=4.77[35]. Using these bulk quantities and $\sigma_c = 0.5e$ per interface unit cell, an electric field of 57.4 mV/Å is obtained, in excellent agreement with the superlattice DFT results.

### C. Chemical charge at interfaces

This agreement indicates that the physically meaningful charge $\sigma_c$ is the one predicted by formal ionic charges, rather than populations. The reason is the same as for dopants in semiconductors, where irrespective of the charge distribution around the dopant, the net charge is the result of counting core charges on one hand and electrons in the valence band on the other. Take the example of phosphorous as a donor in bulk silicon. Its +5 core is surrounded by the same set of bonds that surrounded the Si +4 core it substitutes. The electron-pair clouds of these bonds are deformed (polarized), of course, but the number of electrons remains. The net effect is that the P donor creates an attractive potential for electrons that corresponds to a charge of $+e$, not an effective charge of any kind, the deformation of the bonds around being described by the dielectric constant of bulk silicon.

These arguments were generalized to interfaces three decades ago[36]. The valence-band electron counting was performed in terms of bands, but it can also be done using Lewis pairs or localized Wannier states. In LAO and STO the valence band corresponds to four Wannier states per oxygen, which gives exactly the same numbers as when using formal charges. The local charge neutrality picture[18] can then be used as the easiest way to see the interface charging, but using formal charges, not effective ones. Whether atoms are chemically more or less ionic depends on the shape and displacement of the Wanniers from the O atom towards the cations, but is irrelevant here. What is relevant is the number of electron pairs and the fact that they localize over lengths much smaller than the interface separation.

### D. Insulator to metal transition

The IMT occurs at the critical thickness of $d_c = \Delta/\mathcal{E}^0$, where $\Delta$ is the gap (STO's), including the ZPE for the confining potential at both interfaces (Fig. 4a). Taking the calculated $\mathcal{E}^0$, our DFT gap for strained STO (1.78eV), and both ZPEs as $\sim$ 0.2 eV, a $d_c$ = 38 Å is obtained, $\sim$ 10 unit cells. This value is sensitive to lateral strain, since $P(\mathcal{E})$ depends on strain (especially for STO, so close to a ferroelectric instability). Indeed, repeating the DFT calculation for 8/8 under the lateral lattice parameter of bulk STO gives conducting interfaces. This effect can be used to sense applied strain on a sample tuned to

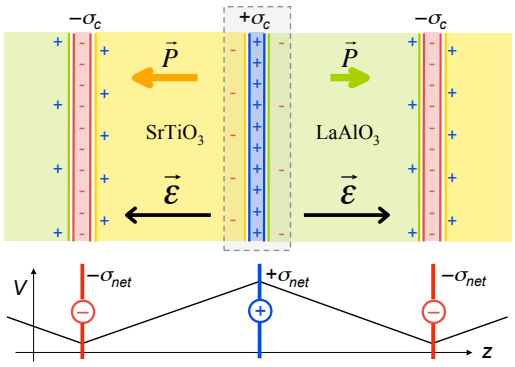


FIG. 3: (Color online) Capacitor-plates model of the LAO/STO superlattice. Above, the plates are indicated by the thinner bands, and $\sigma_c$ indicates the charge of chemical origin attached to each, which is equal but of opposite sign for alternating interfaces. The box around the central plate indicates the surfaces for integration of Gauss's law. The lower panel shows the net electrostatic potential $V$ for the system, which can be seen as arising from plates with $\sigma_{\rm net} = \sigma_c - P_{\rm LAO} - P_{\rm STO}$, the latter $P_{\rm LAO}$ and $P_{\rm STO}$ referring to the magnitude of the respective polarizations (notice that $V$ has opposite sign to what shown in the left panel of Fig. 2, which is $qV$).

be close to the IMT (a piezoresistance device).

Beyond the IMT, a constant density of states for holes and electrons is assumed, modeling 2D parabolic bands. Considering electron transfer from the $p$ to the $n$ interface, equation (1) becomes

$$\sigma_c - P_{\rm LAO} - P_{\rm STO} - (\mathcal{E}d - \Delta)D = 2\epsilon_0\mathcal{E} \tag{3}$$

where $d$ is the interface separation, $\mathcal{E}$ the modified field, and $D$ the density of states (taking equal effective masses for electrons and holes). Proceeding as for equation 2,

$$\mathcal{E} = (\sigma_c + D\Delta - P^0_{\rm STO})/(\epsilon_0\kappa + Dd). \tag{4}$$

The electric field vanishes as $1/d$ for large separations, the charge transferred tending to compensate the chemical charge. In our case, $D\Delta \gg \sigma_c$, and thus $\mathcal{E}/\mathcal{E}^0 \sim d_c/d$, i.e. the voltage drop is essentially pinned by the gap.

### E. Extending the model to other systems

Consider now the model for other systems. Take a superlattice with thicker layers for LAO than for STO (Fig. 4c). It is analogous to a frozen ⟨111⟩ LO phonon in NaCl: the

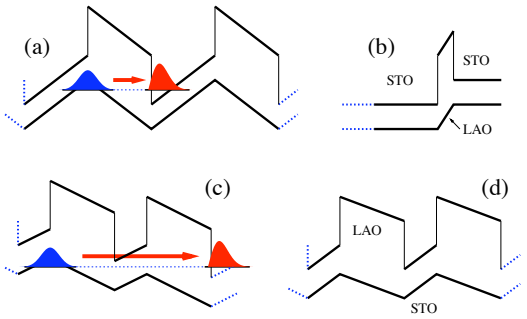


FIG. 4: (Color online) Model band gap versus $z$ for a superlattice with equal thicknesses (a), the thin film sample of ref.[2] (b), and a superlattice with different thicknesses with open (c) and periodic (d) boundary conditions. In (a) and (c) the arrow indicates the charge transfer leading to electron (red) and hole (blue) 2D gases. In both cases the thicknesses depicted give the onset of the charge transfer, corresponding to the insulator to metal transition.

different separations of the charged planes gives a net electric field. PBC remove it as if putting the system between shorted metal plates (Fig. 4d). It is as a ferroelectric, except that switching the spontaneous polarization demands changing the thicknesses. Note that with PBC and thinner STO, $\mathcal{E}_{\rm STO} > \mathcal{E}_{\rm LAO}$. Without shorted plates the system is unstable to the appearance of 2DEGs (Fig. 4c).

The $d_c$ found experimentally on the non-repeated system of ref.[2] is much smaller than our superlattice result. They have one LAO layer interfacing $n$ to the STO substrate and $p$ to an STO overlayer (Fig. 4b). The field is zero in the substrate and overlayer, the $p$ and $n$ interfaces defining a capacitor only screened by LAO. Thus, $\mathcal{E} = \sigma_c/\epsilon_0(1+\chi_{\rm LAO})$, more than twice as large as $\mathcal{E}^0$ of equation 2, giving the observed smaller $d_c$. A similar model has been very recently described for one single $n$ interface[37].

## IV. FINAL REMARKS AND SUMMARY

The electron-hole interactions among 2D gases should establish excitons. Achievable exciton densities are favorable for exciton condensation, the optimal density being[19] $n_{opt} = (\pi a_0^2)^{-1}$, with $a_0^2 \approx (a_B\epsilon/m^*)^2 + d^2$ (Bohr radius, dielectric constant and effective mass, respectively). For our system $n_{opt} \approx 0.002e$/cell, well within range ($n_{12/12} = 0.073e$/cell).

The IMT is affected by the presence of O vacancies. Each donates two electrons to the $n$ interface giving rise to a 2DEG. Their appearance and location depends on their stability and on kinetic effects like electromigration and sample-growth history. Taking stability

arguments only, the IMT via vacancies would happen when $\mathcal{E}^0 d \geq \mu_O/2$, with $\mathcal{E}^0$ as in equation 2 and $\mu_O$ the formation energy of an O vacancy at the $p$ interface, which depends on the oxygen chemical potential at growth conditions.

In summary, the agreement between DFT and the model shows that it contains the relevant physics of these superlattices, pointing to new science and applications by changing relative thicknesses, substrates, and stress.

**Acknowledgments**

We thank H. Y. Hwang, J. F. Scott, P. Ordejon, G. Catalan, N. D. Mathur, J. Junquera, W. E. Pickett and M. A. Carpenter for insightful discussions. We acknowledge support through EPSRC and the computing resources through the HPC facility in Cambridge.

---

[1] A. Ohtomo and H. Hwang, Nature **427**, 423 (2004).

[2] M. Huijben, G. Rijnders, D. Blank, S. Bals, S. Van Aert, J. Verbeeck, G. Van Tendeloo, A. Brinkman, and H. Hilgenkamp, Nat. Mater. **5**, 556 (2006).

[3] N. Nakagawa, H. Hwang, and D. Muller, Nat. Mater. **5**, 204 (2006).

[4] S. A. Pauli and P. R. Willmott, J. Phys.: Condens. Matter **20**, 264012 (2008).

[5] N. Reyren, S. Thiel, A. D. Caviglia, L. F. Kourkoutis, G. Hammerl, C. Richter, C. W. Schneider, T. Kopp, A.-S. Ruetschi, D. Jaccard, et al., Science **317**, 1196 (2007).

[6] S. Thiel, G. Hammerl, A. Schmehl, C. W. Schneider, and J. Mannhart, Science **313**, 1942 (2006).

[7] J. M. Albina, M. Mrovec, B. Meyer, and C. Elsasser, Phys. Rev. B **76**, 165103 (2007).

[8] S. Gemming and G. Seifert, Acta Mater. **54**, 4299 (2006).

[9] K. Janicka, J. P. Velev, and E. Y. Tsymbal, Phys. Rev. Lett. **102**, 106803 (2009).

[10] P. Larson, Z. S. Popovic, and S. Satpathy, Phys. Rev. B **77**, 245122 (2008).

[11] J. Lee and A. A. Demkov, Phys. Rev. B **78**, 193104 (2008).

[12] M. S. Park, S. H. Rhim, and A. J. Freeman, Phys. Rev. B **74**, 205416 (2006).

[13] R. Pentcheva and W. E. Pickett, Phys. Rev. B **74**, 035112 (2006).

[14] R. Pentcheva and W. E. Pickett, Phys. Rev. B **78**, 205106 (2008).

[15] R. Pentcheva and W. E. Pickett, Phys. Rev. Lett. **102**, 107602 (2009).

[16] Z. S. Popovic, S. Satpathy, and R. M. Martin, Phys. Rev. Lett. **101**, 256801 (2008).

[17] H. Chen, A. M. Kolpak, and S. Ismail-Beigi, Phys. Rev. B **79**, 161402(R) (2009).

[18] J. Goniakowski, F. Finocchi, and C. Noguera, Rep. Progr. Phys. **71**, 016501 (2008).

[19] P. B. Littlewood and X. Zhu, Physica Scripta **T68**, 56 (1996).

[20] M. Basletic, J. L. Maurice, C. Carretero, G. Herranz, O. Copie, M. Bibes, E. Jacquet, K. Bouzehouane, S. Fusil, and A. Barthelemy, Nat. Mater. **7**, 621 (2008).

[21] D. M. Ceperley and B. J. Alder, Phys. Rev. Lett. **45**, 566 (1980).

[22] P. Ordejon, E. Artacho, and J. M. Soler, Phys. Rev. B **53**, R10441 (1996).

[23] J. Soler, E. Artacho, J. Gale, A. Garcia, J. Junquera, P. Ordejon, and D. Sanchez-Portal, J. Phys.: Condens. Matter **14**, 2745 (2002).

[24] N. Troullier and J. L. Martins, Phys. Rev. B **43**, 1993 (1991).

[25] E. Anglada, J. M. Soler, J. Junquera, and E. Artacho, Phys. Rev. B **66**, 205101 (2002).

[26] J. Moreno and J. M. Soler, Phys. Rev. B **45**, 13891 (1992).

[27] A. Baldereschi, S. Baroni, and R. Resta, Phys. Rev. Lett. **61**, 734 (1988).

[28] L. J. Sham and M. Schlüter, Phys. Rev. Lett. **51**, 1888 (1983).

[29] Q. Wu and T. Van Voorhis, J. Phys. Chem. A **110**, 9212 (2006).

[30] J. Haeni, P. Irvin, W. Chang, R. Uecker, P. Reiche, Y. Li, S. Choudhury, W. Tian, M. Hawley, B. Craigo, et al., Nature **430**, 758 (2004).

[31] A. Antons, J. B. Neaton, K. M. Rabe, and D. Vanderbilt, Phys. Rev. B **71**, 024102 (2005).

[32] R. D. King-Smith and D. Vanderbilt, Phys. Rev. B **47**, 1651 (1993).

[33] D. Fernandez-Torre, R. Escribano, T. Archer, J. Pruneda, and E. Artacho, J. Phys. Chem. A **108**, 10535 (2004).

[34] W. Zhong, R. D. King-Smith, and D. Vanderbilt, Phys. Rev. Lett. **72**, 3618 (1994).

[35] P. Delugas, V. Fiorentini, and A. Filippetti, Phys. Rev. B **71**, 134302 (2005).

[36] G. A. Baraff, J. A. Appelbaum, and D. R. Hamann, Phys. Rev. Lett. **38**, 237 (1977).

[37] W.-J. Son, E. Cho, B. Lee, J. Lee, and S. Han, Phys. Rev. B **79**, 245411 (2009).

[38] Z. S. Popovic and S. Satpathy, Phys. Rev. Lett **94**, 176805 (2005).

[39] Ref. 38 solves electron confinement in a V-shaped potential. Our 2DEG states are confined by different physics (Fig. 4a) and for a different system.